PNAS
www.pnas.org

Supplementary Information for

Unbalanced bidirectional radial stiffness gradients within the organ of Corti promoted by TRIOBP

Hesam Babahosseini[a,1], Inna A. Belyantseva[b,1], Rizwan Yousaf[b], Risa Tona[b], Shadan Hadi[c], Sayaka Inagaki[b], Elizabeth Wilson[b], Shin-ichiro Kitajiri[d], Gregory I. Frolenkov[c], Thomas B. Friedman[b], Alexander X. Cartagena-Rivera[a,2]

[a] Section on Mechanobiology, National Institute of Biomedical Imaging and Bioengineering, National Institutes of Health

[b] Laboratory of Molecular Genetics, National Institute on Deafness and Other Communication Disorders, National Institutes of Health

[c] Department of Physiology, University of Kentucky

[d] Department of Otolaryngology-Head and Neck Surgery, Kyoto University Graduate School of Medicine

[1] Co-first authors

[2] Corresponding Author: Alexander X. Cartagena-Rivera
Email: cartagenariveax@nih.gov

This PDF file includes:

Supplementary Materials and Methods
Figures S1 to S5
Tables S1 to S3
SI References

Supplementary Materials and Methods

Generation of Mouse Models and Genotyping. Generation of different TRIOBP-5 deficient mouse models such as *Triobp*$^{\Delta Ex9\text{-}10/\Delta Ex9\text{-}10}$ was described in Katsuno *et al.* (1). Briefly, we deleted the genomic sequence from exons 9 to 10 of *Triobp* (1), which were replaced by a nLacZ reporter in frame with the upstream protein sequence of mouse TRIOBP. The deletion encompasses most of the sequence of exon 9 and exon 10 except first 7 bp of exon 9 and 1 base at the 3' end of exon 10. For construction of the targeting vector, an 8 kb 5' arm and a 4 kb 3' arm were obtained from clone RP23-414K1 (BACPAC Resources Center, CA). TT2 embryonic stem (ES) cells (2) were electroporated with the NotI-linearized targeting vector, and ES clones were screened for homologous recombination events. Using specific probes (5' probe: 5'-CTACCCAGTCAGGCTTTGTTTTGTGGC-3' and 5'- GCCAATGTGAACTGCTTAACTC-3', 3' probe: 5'-CTTGGTTTTTAATGTTAGAACCAGATTGGC-3' and 5'-CTAACCATCAGCTCATTTCTTTGAG-3'), PCR-positive ES cell clones were evaluated by Southern blot analyses. Germ-line transmission of the targeted allele was obtained from three lines of chimeric mice produced from ES cell clones #18, #20 and #23. Mice with the deletion of exons 9 and 10 are designated *Triobp*$^{\Delta Ex9\text{-}10}$ in this manuscript, while the JAX nomenclature committee designated this allele *Triobp*^{tm1Sik} (MGI:6189198) with the accession number of CDB0844K assigned by the Riken, http://www2.clst.riken.jp/arg/mutant%20mice%20list.html. *Triobp*^{tm1Sik} mutant mice are available from the JAX Laboratory.

For TRIOBP-4/5 (*Triobp*$^{\Delta Ex8/\Delta Ex8}$) deficient mouse model, exon 8 of *Triobp* was deleted by using a reported methodology (3). nBLUEneo and DT-A (B.DEST) vectors were provided by Dr. Ikeya. The 5' arm (8-kb) and 3' arm (4-kb) of the targeting vector were obtained from clone RP23-414K1 (BACPAC Resources Center, CA). Except for the first 5 bp, all of the sequence of *Triobp* exon 8 (2,288 bp) was removed and a nLacZ reporter cassette inserted in-frame with the upstream protein sequence of *Triobp*. Bruce4 ES cells were electroporated with NotI-linearized targeting vector, and 1056 ES clones were screened for homologous recombination events. PCR-positive ES cell clones were evaluated by Southern blot analyses. Two independent ES cell clones produced chimeric mice. Heterozygotes for the targeted allele were obtained from both lines. Genotyping for *Triobp*$^{\Delta Ex8/\Delta Ex8}$ mice was performed with the following three primers in a single PCR reaction; common forward primer-P1 (Ex8.F3): 5'-CAGGCAACAATGTCTTGGCG-3'; WT reverse primer-P2 (Ex8.WTR3): 5'-GGTTCTGTTGAGAGAGGAGTCTTGG-3'; mutant reverse primer-P3 (Ex8.KOR1): 5'- TGGGTAACGCCAGGGTTTTC-3'. Amplimers using the three PCR primers are 645 bp for WT allele and 338 bp for ΔEx8 allele. Briefly, PCR conditions involved an initial denaturation at 94°C for 2 minutes, then 94°C for 30 seconds, 58°C for 30 seconds, 68°C for 1 minute, which was repeated for 35 cycles with a final extension at 68°C for 10 minutes.

In Situ Hybridization Using RNAscope Probes. *In situ* hybridizations were performed using RNAscope Multiplex Fluorescent V2 assay (Advanced Cell Diagnostics (ACD), Newark, CA) with following probes. The Probe-Mm-Triobp-O1 that targeted the region from nucleotide 387 to 1288 (NM_001039155.1) was used to detect both *Triobp-4* and *Triobp-5* mRNAs. The Probe-Mm-Triobp-O2-C3 targeted the region from nucleotide 3860 to 4773 of NM_138579.4 and was used to detect only *Triobp*-5 mRNA. The Probe-Mm-Triobp-O3 targeted the region from nucleotide 154 to 1170 of NM_001024716.1 and was used to detect both *Triobp*-1 and *Triobp-5*. As a positive control, Probe-Mm-Myo7a-C2 targeted the region from nucleotide 1365 to 2453, NM_001256081.1 of *Myo7a* mRNA was used to label IHCs and OHCs. Cochleae from C57BL/6J wild-type mice at P6 and P14 were fixed overnight at 4ºC in 4% paraformaldehyde (Electron Microscopy Sciences, Hatfield, PA) in 1x phosphate buffered saline (PBS). Fixed P14 cochleae were decalcified in 10% ethylenediaminetetraacetic acid for 5 days. Then, cochleae were cryopreserved in 15% sucrose in 1x PBS overnight at 4ºC and then in 30% sucrose in 1X PBS overnight at 4ºC. Each cochlea was embedded and frozen in Super Cryoembedding Medium (Section-Lab, Hiroshima, Japan). Frozen cochleae were sectioned at a thickness of 12µm using a CM3050S cryostat microtome (Leica, Vienna, Austria). Images were taken with an LSM 880 confocal microscope equipped with 63x and 40x objectives (Carl Zeiss Microscopy, Thornwood, NY).

Quantitative Droplet Digital PCR. In order to evaluate the expression profile of different *Triobp* mRNA isoforms, whole inner ears were dissected from wild-type *Triobp*$^{+/+}$, heterozygous *Triobp*$^{\Delta Ex9\text{-}10/+}$ and homozygous *Triobp*$^{\Delta Ex9\text{-}10/\Delta Ex9\text{-}10}$ mice at P6. Total RNA was extracted using TRIzol (Invitrogen, USA) followed by first-strand complementary DNA (cDNA) synthesis using a SuperScript™ RT-PCR kit (Invitrogen, USA) according to manufacturer instructions. TaqMan probes for different isoforms of *Triobp* were designed (*SI Appendix,* Fig. S1A), *Triobp-1* primers spanned the junction between exon 1b, which is unique for *Triobp1* mRNA, to exon 13, with probe designed over the exon junction [Triobp_1-FWD GGGAAGGGCTGGAGCTA; Triobp_1-REV AGATTGACATCCATCCTTTCTTGA; Triobp_1-PRB /56FAM/CATGACGCC/ZEN/CGATCTGCTCAACT/3IABkFQ/]. Whereas for detecting *Triobp-5*, the primers were designed spanning the junction from exon 8 to exon 9 and the TaqMan probe designed over the junction [Triobp_5-FWD AGGTGGAGCGCCTCTTC; Triobp_5-REV AAGTTGGCTCTGAGCTTGG; Triobp_5-PRB /56-FAM/AAGAGCGCA/ZEN/GGAAATCGGAGGC/3IABkFQ/]. To detect cDNA synthesized from*Triobp-4* mRNA, a forward primer was designed in exon 8, and the reverse primer was located in sequence of the exon 8 UTR unique only to *Triobp-4* [Triobp_4-FWD GCAAGAGCGCAGGTGAG; Triobp_4-REV CAGCAGGGCTTGAACTCTT; Triobp_4-PRB/56-FAM/TGGAACTTT/ZEN/CCAACTGTTCTCCTCCC/3IABkFQ/] (*SI Appendix,* Fig. S1A).

The expression of the *Triobp* alternative splice isoforms was quantified using a QX200 ddPCR System (Bio-Rad, USA) according to the manufacturer's instructions. Briefly, a 20 µL ddPCR reaction comprised of 2x ddPCR Supermix for Probes (no dUTP) (Bio-Rad, USA), 20x TaqMan assay primer-probe mix and cDNA sample. Droplets were generated using the Automated Droplet Generator (Bio-Rad, USA). The PCR plate was subsequently heat-sealed with pierceable foil using a PX1 PCR plate sealer (Bio-Rad, USA) and then amplified in a Veriti thermal cycler (Applied Biosystems, USA) using the following amplification cycling conditions, with initial enzyme activation at 95°C for 10min, followed by 40 cycles of denaturation at 94°C for 30 sec and an annealing/extension step at 60°C for 1 min. Final enzyme inactivation at 98°C for 10 min and held at 4°C until the next step. After amplification, the 96-well plate was fixed in a plate holder and placed into the QX200 Droplet Reader (Bio-Rad, USA) and droplets from each well of the plate were read automatically. QuantaSoft analysis software (Bio-Rad, USA) was used to analyze ddPCR data and for the quantification of the target molecule per 1 µl of PCR reaction.

Electron Tomography with Focused Ion Beam Serial Sectioning and Scanning Electron Microscopy Imaging (FIB-SEM). Cochleae from wild-type *Triobp*$^{+/+}$, heterozygous *Triobp*$^{\Delta Ex9\text{-}10/+}$ and homozygous *Triobp*$^{\Delta Ex9\text{-}10/\Delta Ex9\text{-}10}$ mice at postnatal day 6 and 7 (P6 and P7) were extracted from temporal bones and gently perfused through the oval window with a solution containing 2.5% glutaraldehyde, 2% paraformaldehyde in 0.1M cacodylate buffer, pH=7.4 (Electron Microscopy Science, cat# 15960-01), and supplemented with 2mM $CaCl_2$ and 1% Tannic acid (Electron Microscopy Sciences, cat# 21710). The cochleae were kept in this fixative overnight at 4°C, and then the fixative was diluted ~1:5 with 0.1M cacodylate buffer and samples were shipped to the University of Kentucky. Then, the organs of Corti were dissected in distilled water with the tectorial membrane kept intact and high-pressure frozen with Leica EM ICE high-pressure freezer. The frozen samples were transferred to Leica EM AFS2 freeze substitution machine and kept in methanol with 1% uranyl acetate at -90°C for 33 hours and then slowly warmed at about 4°C per hour to -45°C. Samples were then washed with fresh 100% methanol for 24 hours at -45°C to fully replace uranyl acetate. Then the methanol was gradually replaced with Lowicryl HM-20 resin (monostep embedding kit, Electron Microscopy Sciences, cat# 14345): 50% Lowicryl (2 hours), 75% Lowicryl (overnight ~21 hours), and 100% Lowicryl (overnight ~24 hours). To ensure that there is no residual methanol, the samples were additionally incubated with fresh 100% Lowicryl for 1 hour. Then, samples were transferred into flat mold with 100% Lowicryl, incubated for additional 24 hours, and polymerized with UV light at -45°C for 27 hours, at 0°C for additional 40 hours, and at 20°C for 48 hours. The resin blocks were trimmed (Leica EM TRIM2) to reach a desired sample distance of 20-50µm from the

upper surface of the block. Samples were then sputter coated with 25 nm of platinum (Electron Microscopy Science, EMS150T ES) and serial sectioned with a focused ion beam at a 20nm step size and imaged in “Slice and View” mode with a backscattered electron detector using the FEI Helios 660 Nanolab system.

Analysis of FIB-SEM stacks. Raw FIB-SEM stacks typically contained several hundreds of images with 6144x4096 pixels with a voxel size of ~2x2x20 nm. They were registered either with a custom MATLAB script or with SIFT registration plugin in ImageJ-2 (Fiji, National Institutes of Health). After 3D median filtering, the stacks were rotated with Interactive Stack Rotation plugin in Fiji in such a way that the field of view became parallel to the feature of interest (upper surface of the cuticular plate for hair cells or reticular lamina for supporting cells). These rotated stacks were used to construct top median Z-projection views of the cell of interest. To reveal microtubules/microfilaments within the outer pillar cells, the stacks were further oriented in such a way that microfilaments/microtubules would align with X-axis and then the stack was rotated 90 degrees along the X-axes, providing a lateral view of these structures. Thus, a starting orientation of the field of view parallel to the cuticular plate of hair cells (or reticular lamina in supporting cells) ensures the match of orientations of resulting Z-projections between the samples.

Immunostaining. P8 and P20 wild-type *Triobp*$^{+/+}$ and homozygous *Triobp*$^{\Delta Ex9\text{-}10/\Delta Ex9\text{-}10}$ mice were used for immunostaining of the organ of Corti with anti-TARA antibody (Proteintech, cat#16124-1-AP) which was developed against an antigen corresponding to the C-terminal sequence of TRIOBP5 identical to TRIOBP-1, as reported (4). We also used antibodies against TRIOBP-4/5 and against TRIOBP-5 as previously described (1, 5). Briefly, for TRIOBP-4/5 and TRIOBP-5 antibodies, organs of Corti were fixed in 2% paraformaldehyde for 30 min at room temperature (RT), microdissected and permeabilized in 0.2% Triton X-100 in 1X PBS for 15 min at RT, washed in 1X PBS and incubate in blocking solution (2% BSA and 5% normal goat serum in 1X PBS) overnight at 4˚C. Next day the samples were transferred to the custom-made primary rabbit polyclonal anti-TRIOBP-5 antibody (1, 5) diluted in blocking solution 1:200 to obtain 5 µg/ml concentration and incubated for 2 hours at RT, followed by 3 X 10 min washes in 1X PBS. Then samples were incubated in secondary anti-rabbit Alexa Fluor 488 or 568 conjugated antibody (Thermo Fisher, Cat # R37118) at 1:400 dilution together with Rhodamine-phalloidin (Thermo Fisher, Cat # R415), phalloidin Atto-390 (Sigma, Cat # C926P04) or FITC-conjugated b-actin (Abcam, Cat # ab6277) at 1:100 dilution in blocking solution for 30 min at RT, followed by 3 X 10 min washes in 1X PBS and mounted on glass slides using ProLong Gold Antifade Mountant (Thermo Fisher, Cat # P36934). Prepared slides were kept in a slide box at 4^{0}C overnight and then examined using a LSM 780 Zeiss confocal microscope equipped with a 63x, 1.4 N.A. oil immersion objective.

Organ of Corti Explant Cultures. Wild-type *Triobp*$^{+/+}$, heterozygous *Triobp*$^{\Delta Ex9\text{-}10/+}$, and homozygous *Triobp*$^{\Delta Ex9\text{-}10/\Delta Ex9\text{-}10}$ mice, as well as heterozygous *Triobp*$^{\Delta Ex8/+}$ and homozygous *Triobp*$^{\Delta Ex8/\Delta Ex8}$ mice were used for explant culture experiments. Three P6 pups of each genotype were sacrificed by decapitation according to the National Institutes of Health Guidelines for Care and Use of Laboratory Animals. The bullae were removed from mouse temporal bones and submerged in cold Leibovitz media (L-15, 21083-027, Life Technologies). The organ of Corti sensory epithelium was microdissected from the cochleae, the tectorial membrane was removed using 27-gauge needle and the entire spiral of the organ of Corti was plated on a glass-bottom petri dish (HBST-5040, Willco Wells) precoated with 10 µl of Cell-Tak (Corning) to immobilize it, and immersed in Leibovitz media (L-15, 21083-027, Life Technologies). The organ of Corti culture was incubated at 37ºC and 5% CO_2 for 15-30 min to achieve firm attachment of the specimen before the PFT-AFM measurements.

PFT-AFM Imaging. PeakForce Tapping mode (PFT-AFM) images were obtained using a Bruker BioScope Catalyst AFM system (Bruker) mounted on an inverted Zeiss Axiovert 200M optical microscope equipped with a 40x objective (0.95 NA, Plan-Apochromat, Zeiss) and a confocal laser scanning microscope (LSM 510 META, Zeiss). During PFT-AFM experiments,

the organ of Corti sensory epithelium explants were maintained at 37°C using a Bruker heated stage and scanned using a probe appropriate for live cell imaging with a tip height of 17 μm, controlled tip radius of 65 nm, and opening angle of 15° (PFQNM-LC, Bruker). The cantilever probes used had spring constant values ranging between 0.06–0.08 N/m and were pre-calibrated by the Bruker AFM system using the thermal tune method. Probes were replaced for each new experiment or more frequently as needed. The images were collected at a scan resolution of 128 × 128 pixels and a scan rate of 0.5 Hz. Each tissue scan lasted ~10 minutes. The driving frequency was set at 500 Hz and the drive amplitude was set up to 850 nm. The peak force setpoint was kept between 800 pN and 1.2 nN. The Young's modulus stiffness maps of the samples were analyzed and extracted via the NanoScope Analysis software (Bruker) using the Sneddon's contact mechanics model in which $\mathrm{F_{Sneddon}} = (8\mathrm{E}\tan\alpha/3\,\pi)\delta^2$, where *F* is the applied force, *α* is the tip half-opening angle, and *δ* is the sample mean indentation (6).

Analysis of Young's Modulus Maps. To extract the Young's modulus for individual cells from elastic modulus maps we combined each respective topography and elastic modulus map to identify each cell type cell-cell boundaries. After defining the cell-cell boundaries manually, we defined a region of interest (ROI) on the apical surface at the center of each cell type. The defined/drawn ROI have dimensions of 1.5 μm x1.5 μm containing a total of 100 points (Young's modulus values) per ROI. We then determined the mean and standard deviation values for each ROI. We decided to select ROIs at the center of each cell type apical surface because we wanted to measure the stiffness of the apical cells' F-actin cortex and cuticular plate, while in addition we wanted to remove the influence of the cell-cell junctions which are stiff structures due to the actomyosin belt structures at cell-cell adherent junctions.

Pivotal Stiffness of Stereocilia. The PFT-AFM experiments produced continuous series of force-distance curves throughout the tested cochlear samples. Discrete raw force-distance curves across the hair cell bundles were acquired and the noncontact virtual deflection tilt (generated by hydrodynamic drag) of the baseline was corrected using NanoScope Analysis software (Bruker). Then, individual force-distance curves were quantitatively analyzed using a custom-made MATLAB-based data processing code to determine the apparent pivotal/point (localized) stiffness, script included in the *SI Appendix, MATLAB script for determination of stereocilia pivotal stiffness*. The pivotal/point stiffness was determined by performing a linear curve fitting process. Thus, the pivotal stiffness is the slope of the force curve. Note, that the PFT-AFM-based hair bundle deflection from the probe-hair bundle contact point was limited to ~200 nm for the force-distance curves to calculate the pointed apparent stiffness. Our measurements were limited to 200 nm of stereocilia deflection because in normal hearing the physiological deflections of hair bundles are between 80 nm to 200 nm (7).

MATLAB Script for Determination of Stereocilia Pivotal Stiffness.

```
clc

clear all

data=dlmread('C:\Users\babahosseinih2\Desktop\Bundle FZ_test-Retract\TRIOBP5
KO_P5_bundlestiffness\PFTQNM Cochlea P5 10_13_2017\Mouse2-
Mut\M2Cell3\1\M2Cell3.000.pfc-B41C_ForceCurveIndex_16147.spm - NanoScope
Analysis.txt','\t',1,0);

%-------------------------------------------------------

piezo_pos=data(:,1);%*1e3;

def_m=data(:,2);


subplot(2,2,1)

plot(piezo_pos,def_m)

xlabel('piezo position (nm)')

ylabel('deflection (nm)')

grid on

title('Cantilever deflection vs. Piezo position')


%-------------------------------------------------------


k=0.073; %nN/nm

Force=k*def_m;

force=max(Force) % applied force


D=(piezo_pos)-(def_m);

indentation=max(D) % caused indentation


subplot(2,2,2)

plot(D,Force)

xlabel('separation distance (nm)')

ylabel('Force (nN)')

title('Force vs. Separation distance')
```

```
grid on
%-------------------------------------------------------------

tol_L_fit=0.55e3; % Lower limit tolerance %guess the seperation distance at initial indentation
point
tol_U_fit=1.535e3;   % Upper limit tolerance

j=1;
for j=1:10

q=1;
for w=1:length(D)

   if D(w) >= tol_L_fit && D(w) <= tol_U_fit
      yy(q)=Force(w);
      xx(q)=D(w);
      q=q+1;
   end
end

PP=polyfit(xx,yy,1); % slope & y-intercept
%z_o=-(PP(2)/PP(1)); % x-intercept

%tol_L_fit=z_o;
z_o=tol_L_fit;

j=j+1;
end

subplot(2,2,3)
plot(xx,yy)
title('Fitting region')
```

```
xlabel('separation distance (nm)')
ylabel('Force (nN)')
grid on

%-------------------------------------------------------------
subplot(2,2,4)
plot(D,Force)
grid on

hold on
plot(z_o,yy(1),'o','Color','green')

r=corrcoef(yy,xx);
r_squared=r(2,1)^2

apparent_k_sample=PP(1)*1e3 % pN/nm
```

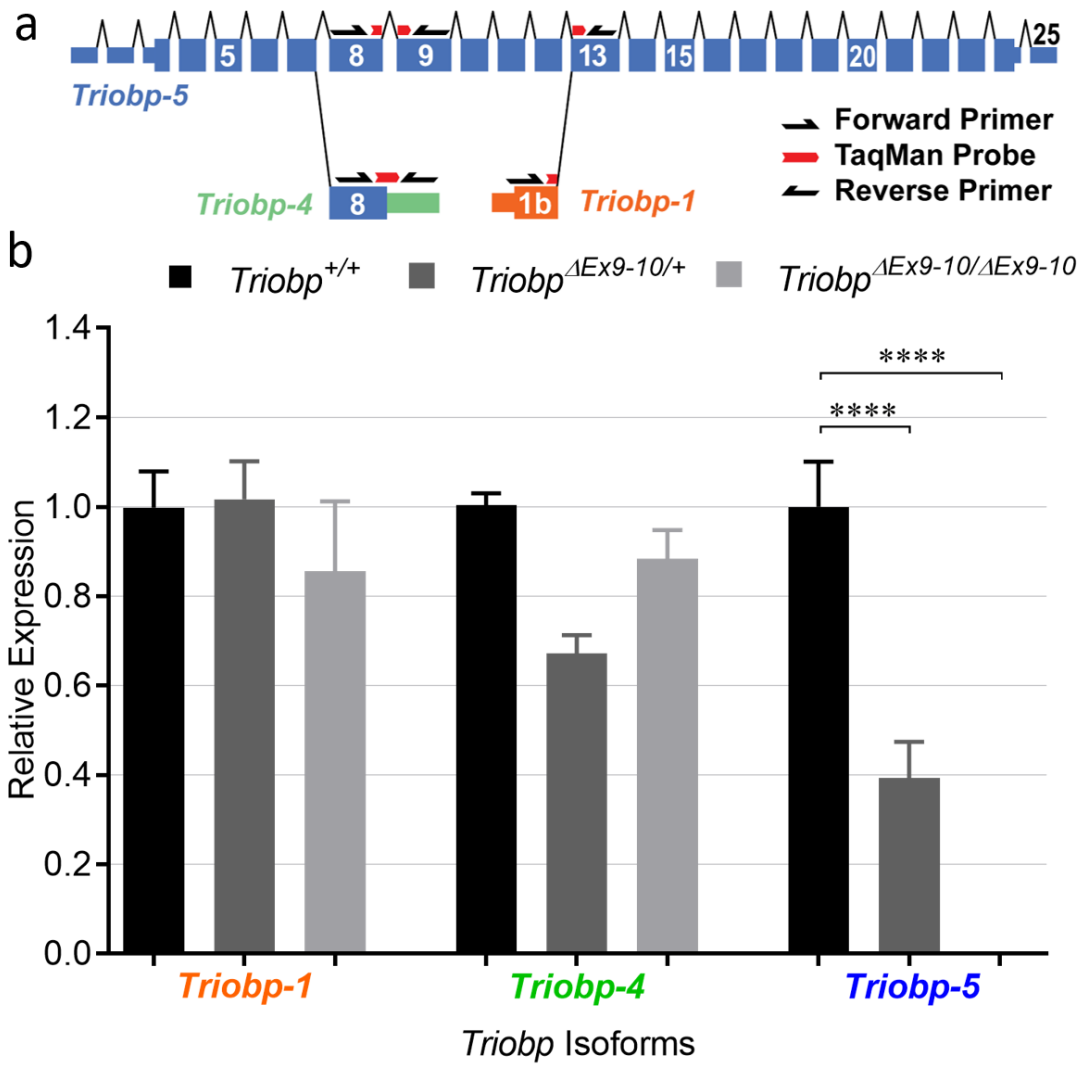

Fig. S1 Expression profile of different isoforms in the *Triobp*$^{\Delta Ex9\text{-}Ex10}$ mouse inner ear at P6. **(A)** TaqMan probes were designed to quantify different isoforms of *Triobp* mRNA. For Triobp-1 primers were designed that flanked the exon junction between exon 1b (orange), which is unique to *Triobp-1* mRNA, and exon 13, with probe designed over the exon junction. Whereas, for Triobp-5, the primers were designed flanking the exon 8 - 9 exon junction, with the probe designed over the spanning junction. To detect cDNA synthesized from *Triobp-4* mRNA, a forward primer was designed in the coding region of exon 8. The reverse primer was located in sequence of the 3' UTR of exon 8 unique only to Triobp-4 (Green). **(B)** Expression levels of three *Triobp* mRNA isoforms (*Triobp-1*, *Triobp-4* and *Triobp-5*) which were measured using ddPCR. There did not appear to be statistically significant difference in expression levels of either *Triobp-1 or Triobp-4* isoforms among the three genotypes. However, the *Triobp-5* expression level was reduced by approximately 40% in heterozygous *Triobp*$^{\Delta Ex9\text{-}10/+}$ mice, a genotype that ablates 2 exons of *Triobp-5* in one genomic copy of the Triobp gene. No mRNA expression of *Triobp-5* was detected in homozygous *Triobp*$^{\Delta Ex9\text{-}10/\ \Delta Ex9\text{-}10}$ mice. Data are represented as mean ± standard error of mean; significant differences between conditions by unpaired two-tailed Student's t-test with Welch's correction indicated as **** P<0.0001.

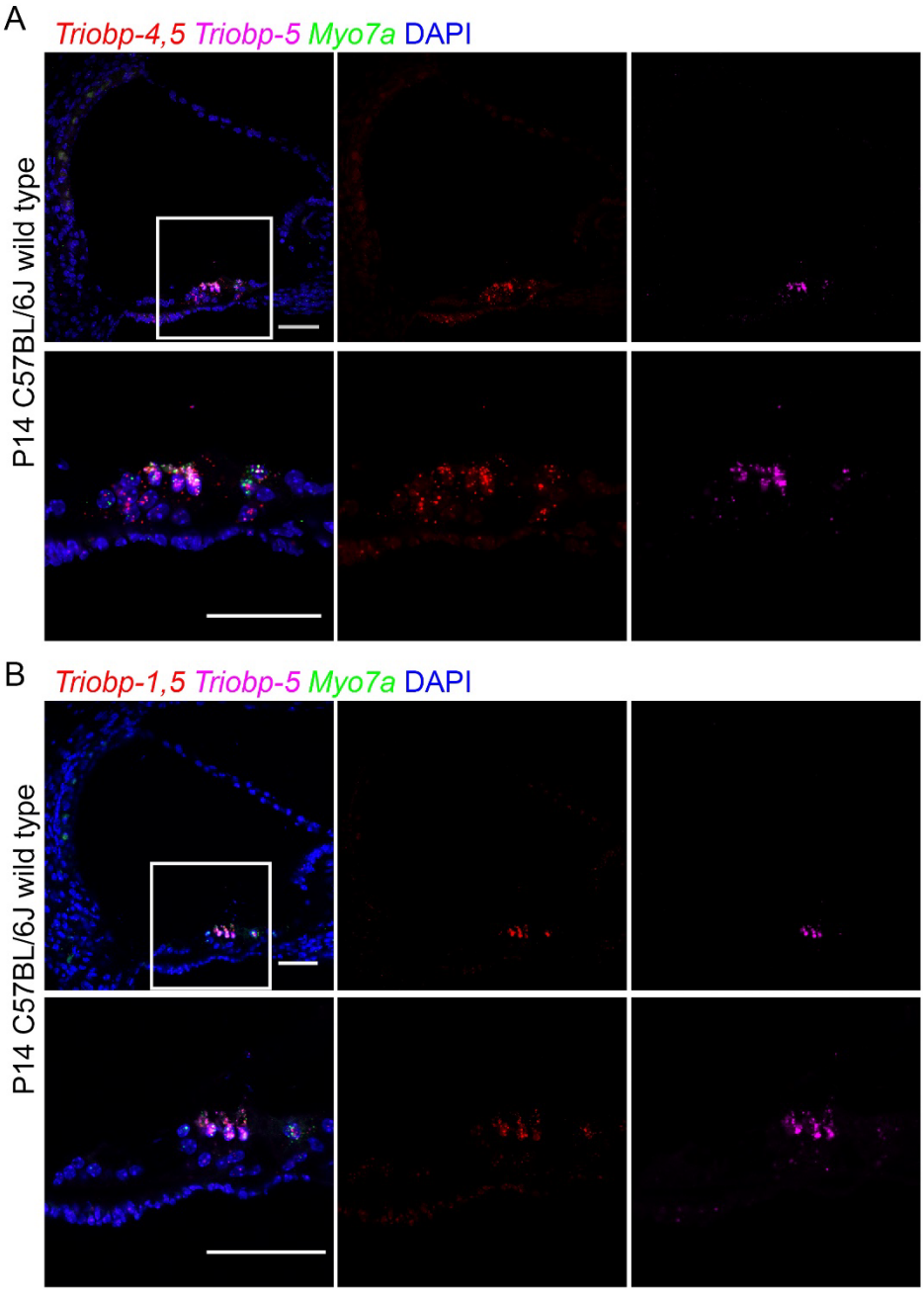

Fig. S2 (related to Figure 2) RNAscope probe *in situ* hybridization in P14 wild-type mouse cochlea. (A) Expression of *Triobp-4 and Triobp-5* mRNAs (*Triobp-4/5*) (red, Probe-Mm-Triobp-O1), *Triobp-5* only mRNA (magenta, Probe-Mm-Triobp-O2-C3) and *Myo7a* mRNA (green, Probe-Mm-Myo7a-C2). *Triobp-4/5* mRNA (red) is expressed in inner and outer hair cells and supporting cells. Whereas mRNA of *Triobp-5* alone is expressed mainly in OHCs. **(B)** Expression of both *Triobp-1 and Triobp-5* mRNA (*Triobp-1/5*) (red, Probe-Mm-Triobp-O3), *Triobp-5* only mRNA (magenta, Probe-Mm-Triobp-O2-C3) and *Myo7a* mRNA (green, Probe-Mm-Myo7a-C2). *Triobp-1/5* mRNA was detected mainly in hair cells. Scale bars are 50 µm.

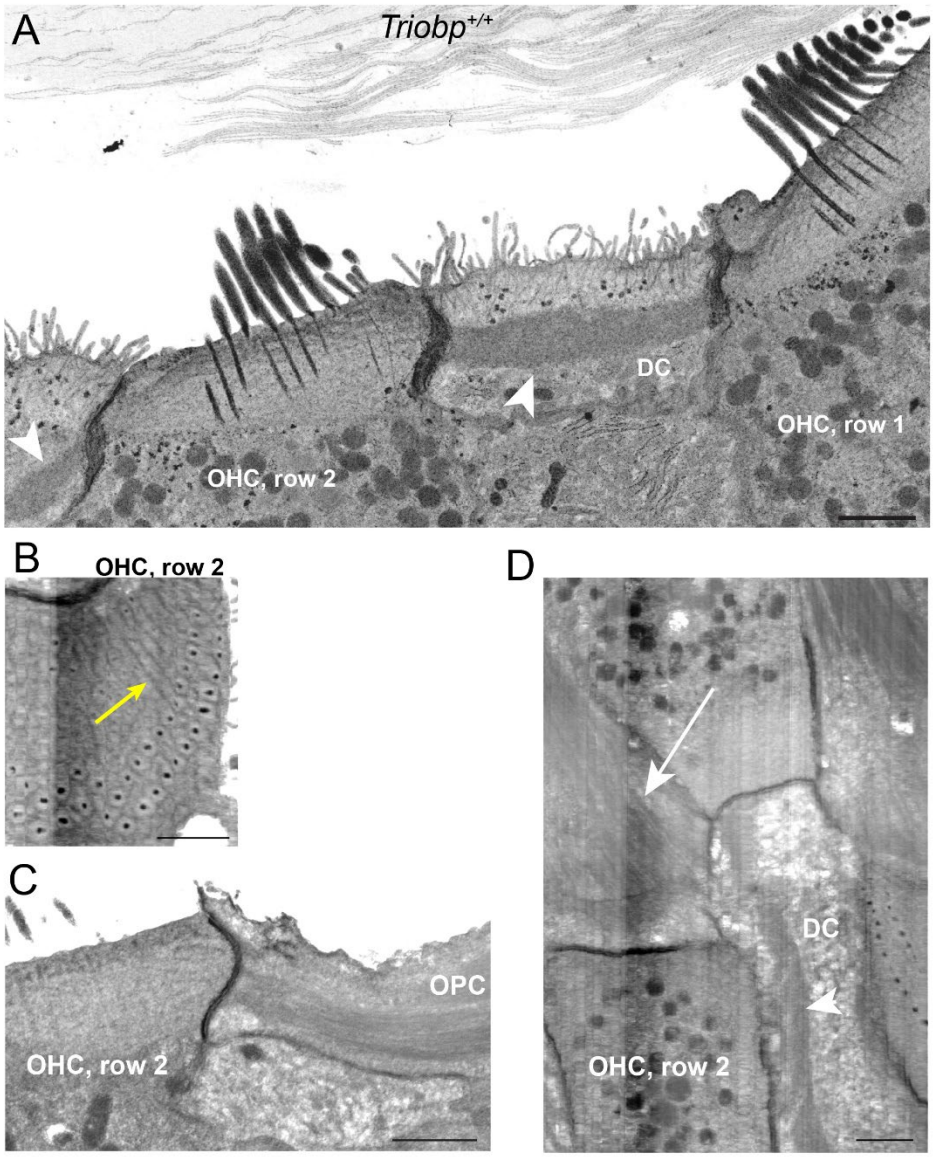

Fig. S3 (related to Figure 4) Microfilaments/microtubules structures in outer hair cells and supporting cells of wild-type *Triobp*$^{+/+}$ mice. (A) Dense microfilamentous structures observed in the apical portion of Deiters' cells (DCs). **(B)** Regular actin "tangles" at the upper surfaces of the OHC cuticular plates, similar to the ones observed in *Triobp*$^{\Delta Ex9\text{-}10/+}$ mice in Fig. 4A (left panel, yellow arrows). The data are representative of four *Triobp*$^{+/+}$ OHCs. **(C)** Lateral view of microfilaments/microtubules in outer pillar cells (OPCs). **(D)** Top view of microfilaments/microtubules in OPCs (white arrow) and actin patches in DCs (arrowhead), similar to the ones observed in *Triobp*$^{\Delta Ex9\text{-}10/+}$ mice in Fig. 4C (left panel). The data are representative of three *Triobp*$^{+/+}$ OPCs and four *Triobp*$^{+/+}$ DCs. Panel (A) shows maximum intensity projection view of a 400 nm-thick FIB-SEM volume, while panels (B-D) show median Z-projections of a 400 nm-thick FIB-SEM volume as in Fig. 4. Vertical darkened strips and lines in panels (B) and (D) occurred due to FIB-SEM data acquisition instability. All scale bars: 1 μm.

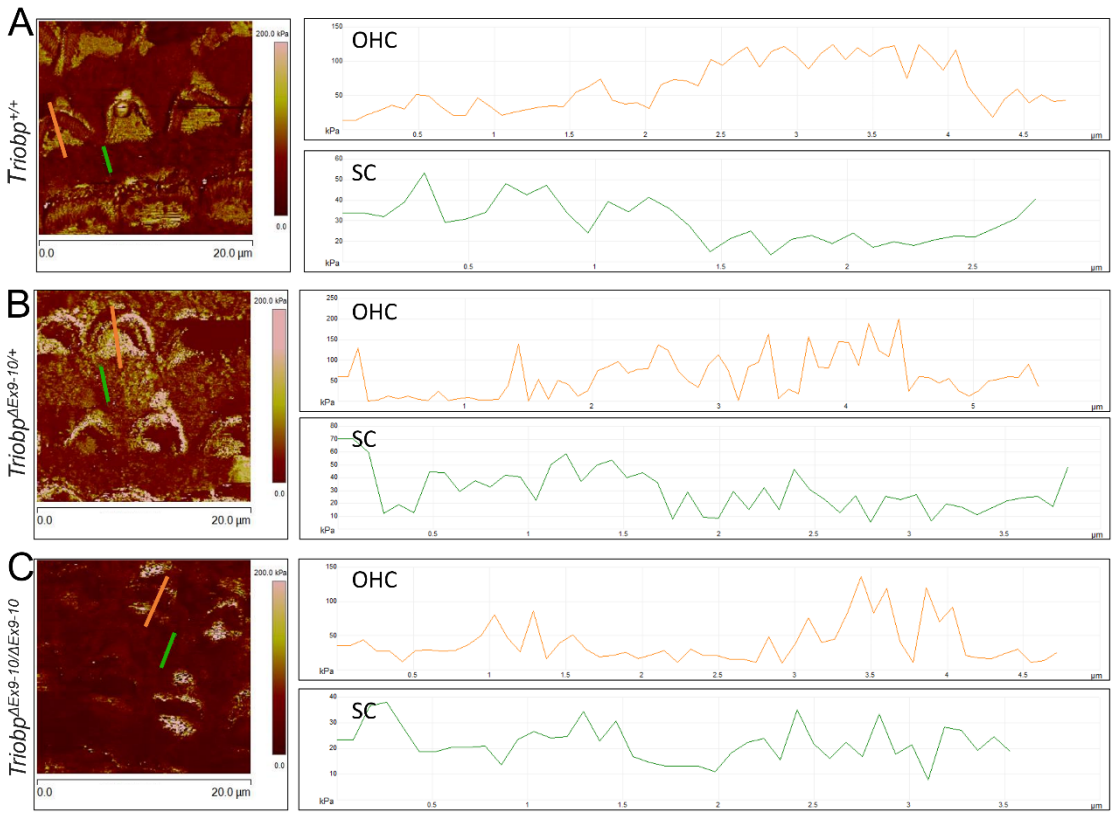

Fig. S4 (related to Figure 5) Extracted line profiles from TRIOBP-5 deficient mice cochlear explants PFT-AFM maps shows nanometer scale variations of apical surface Young's modulus on outer hair cells and supporting cells. Stiffness maps and line profiles of the organ of Corti explants for wild-type *Triobp*$^{+/+}$ **(A)**, heterozygous *Triobp*$^{\Delta Ex9\text{-}10/+}$ **(B)**, and homozygous *Triobp*$^{\Delta Ex9\text{-}10/\Delta Ex9\text{-}10}$ mice **(C)**. The orange and green line profiles represent stiffness data of an outer hair cell and a supporting cell, respectively.

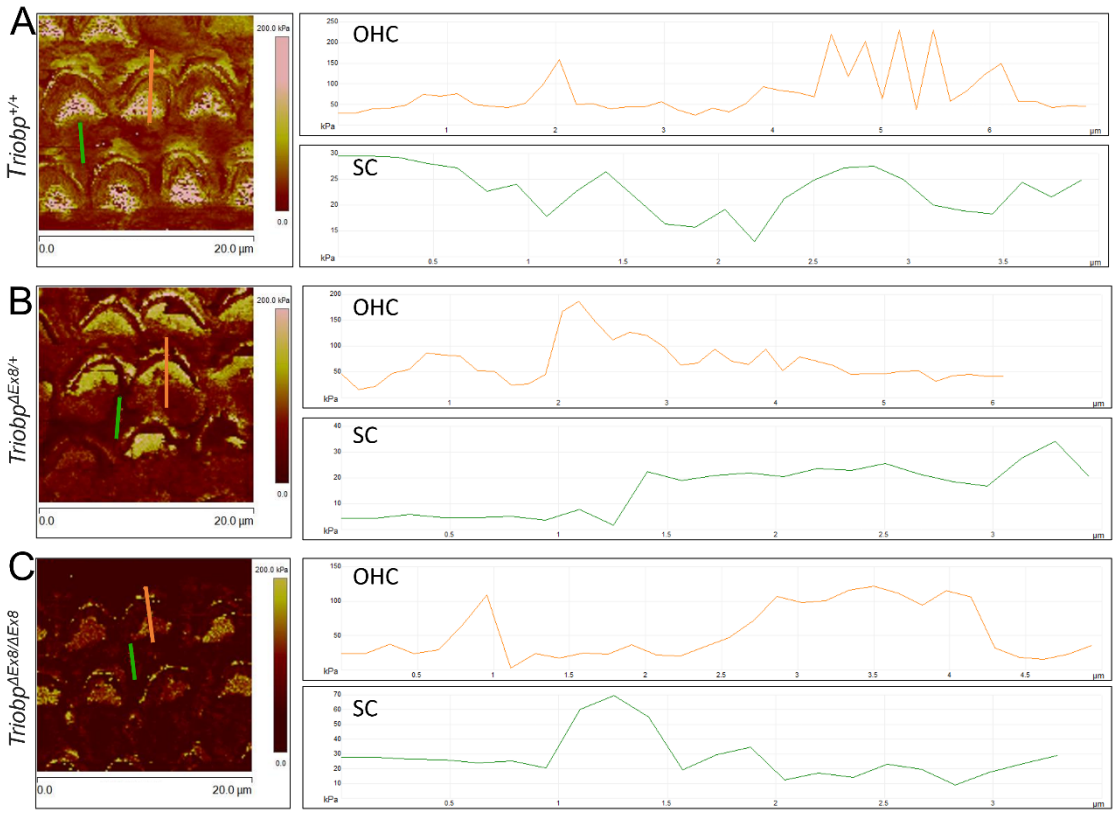

Fig. S5 (related to Figure 6) Extracted line profiles from TRIOBP-4/5 deficient mice cochlear explants PFT-AFM maps shows nanometer scale variations of apical surface Young's modulus on outer hair cells and supporting cells. Stiffness maps and line profiles of the organ of Corti explants for wild-type *Triobp*$^{+/+}$ **(A)**, heterozygous *Triobp*$^{\Delta Ex8/+}$ **(B)**, and homozygous *Triobp*$^{\Delta Ex8/\Delta Ex8}$ mice **(C)**. The orange and green line profiles represent stiffness data of an outer hair cell and a supporting cell, respectively.

Table S1 (related to Figure 5) Summarized measurements for the Young's modulus (kPa) of the organ of Corti middle turn apical surface of supporting cells and cuticular plate of hair cells and stiffness (slope, pN/nm) of stereocilia within hair bundles obtained from live P5-P6 explants for wild-type *Triobp*$^{+/+}$, heterozygous *Triobp*$^{\Delta Ex9\text{-}10/+}$, and homozygous *Triobp*$^{\Delta Ex9\text{-}10/\Delta Ex9\text{-}10}$ mice.

Measured Area	Cell Type	*Triobp*$^{+/+}$	*Triobp*$^{\Delta Ex9\text{-}10/+}$	*Triobp*$^{\Delta Ex9\text{-}10/\Delta Ex9\text{-}10}$
Supporting Cells Apical Phalangeal Surfaces	IPCs	32±23 (n=38)	20±8 (n=41)	11±4 (n=22)
	OPCs	37±17 (n=48)	28±11 (n=55)	18±6 (n=46)
	DCs1	63±36 (n=53)	39±11 (n=52)	22±6 (n=60)
	DCs2	67±36 (n=34)	42±13 (n=26)	25±7 (n=32)
Hair Cells Cuticular Plates	OHCs1	142±58 (n=34)	100±47 (n=29)	93±42 (n=27)
	OHCs2	120±58 (n=50)	93±48 (n=35)	88±39 (n=52)
	OHCs3	93±43 (n=31)	88±40 (n=23)	87±32 (n=36)
Stereocilia Bundles	OHCs1	15±7 (n=41)	14±5 (n=13)	11±3 (n=18)
	OHCs2	15±6 (n=32)	13±6 (n=18)	10±5 (n=30)
	OHCs3	14±3 (n=9)	12±5 (n=13)	9±4 (n=13)

*mean (kPa) ± standard deviation and n is the number of cells. IPCs, Inner pillar cells; OPCs, Outer pillar cells; DC, Deiters' cells; OHCs, Outer hair cells. Represented data were acquired in replicates for *Triobp*$^{+/+}$ wild-type mice (4 animals), *Triobp*$^{\Delta Ex9\text{-}10/+}$ heterozygous mice (5 animals), and *Triobp*$^{\Delta Ex9\text{-}10/\Delta Ex9\text{-}10}$ homozygous mice (5 animals).

Table S2 (related to Figure 6) Summarized measurements for the Young's modulus (kPa) of the organ of Corti middle turn apical surface of supporting cells and cuticular plate of hair cells and stiffness (slope, pN/nm) of stereocilia within hair bundles obtained from live P5-P6 explants for wild-type *Triobp*$^{+/+}$, heterozygous *Triobp*$^{\Delta Ex8/+}$, and homozygous *Triobp*$^{\Delta Ex8/\Delta Ex8}$ mice.

Measured Area	Cell Type	*Triobp*$^{+/+}$	*Triobp*$^{\Delta Ex8/+}$	*Triobp*$^{\Delta Ex8/\Delta Ex8}$
Supporting Cells Apical Phalangeal Surfaces	IPCs	32±23 (n=38)	30±10 (n=18)	15±10 (n=32)
	OPCs	37±17 (n=48)	27±9 (n=24)	23±18 (n=47)
	DCs1	63±36 (n=53)	36±7 (n=21)	27±16 (n=52)
	DCs2	67±36 (n=34)	47±16 (n=15)	31±18 (n=38)
Hair Cells Cuticular Plates	OHCs1	142±58 (n=34)	103±29 (n=15)	58±37 (n=35)
	OHCs2	120±58 (n=50)	69±15 (n=20)	68±34 (n=51)
	OHCs3	93±43 (n=31)	74±20 (n=18)	71±33 (n=34)
Stereocilia Bundles	OHCs1	15±7 (n=41)	16±3 (n=24)	10±2 (n=25)
	OHCs2	15±6 (n=32)	15±2 (n=25)	9±2 (n=38)
	OHCs3	14±3 (n=9)	15±3 (n=7)	9±3 (n=13)

*mean (kPa) ± standard deviation and n is the number of cells. IPCs, Inner pillar cells; OPCs, Outer pillar cells; DC, Deiters' cells; OHCs, Outer hair cells. Represented data were acquired in replicates for *Triobp*$^{+/+}$ wild-type mice (4 animals), *Triobp*$^{\Delta Ex8/+}$ heterozygous mice 5 animals), and *Triobp*$^{\Delta Ex8/\Delta Ex8}$ homozygous mice (5 animals).

Table S3 (related to Figure 7) Summary of radial gradients in Young's modulus values against cell positions within the organ of Corti reticular lamina (slope; E/radial position) of supporting and hair cells obtained from live P5-P6 explants for wild-type *Triobp*$^{+/+}$, heterozygous *Triobp*$^{\Delta Ex9\text{-}10/+}$, and *Triobp*$^{\Delta Ex8/+}$, homozygous *Triobp*$^{\Delta Ex9\text{-}10/\Delta Ex9\text{-}10}$, and *Triobp*$^{\Delta Ex8/\Delta Ex8}$ mice.

Cell Type	Hair Cells	Supporting Cells
Triobp$^{+/+}$	-29±20 (n=4)	17±6 (n=4)
Triobp$^{\Delta Ex9\text{-}10/+}$	-7±22 (n=5)	10±1 (n=5)
Triobp$^{\Delta Ex8/+}$	-10±11 (n=5)	7±0.2 (n=5)
Triobp$^{\Delta Ex9\text{-}10/\Delta Ex9\text{-}10}$	-9±10 (n=5)	5±0.5 (n=5)
Triobp$^{\Delta Ex8/\Delta Ex8}$	4±14 (n=5)	4±1 (n=5)

*mean ± standard error of the mean. n is the number of animals.

SI References

1. T. Katsuno *et al.*, TRIOBP-5 sculpts stereocilia rootlets and stiffens supporting cells enabling hearing. *JCI Insight* 4 (2019).

2. M. Ikeya *et al.*, Gene disruption/knock-in analysis of mONT3: vector construction by employing both in vivo and in vitro recombinations. *Int. J. Dev. Biol.* 49, 807-823 (2005).

3. T. Yagi *et al.*, A Novel ES Cell Line, TT2, with High Germline-Differentiating Potency. *Analytical Biochemistry* 214, 70-76 (1993).

4. J. F. Krey *et al.*, ANKRD24 organizes TRIOBP to reinforce stereocilia insertion points. *Journal of Cell Biology* 221 (2022).

5. S. Kitajiri *et al.*, Actin-bundling protein TRIOBP forms resilient rootlets of hair cell stereocilia essential for hearing. *Cell* 141, 786-798 (2010).

6. I. N. Sneddon, *Fourier transforms*, Dover books on mathematics (Dover Publications, New York, 1995), pp. xii, 542 p.

7. A. J. Ricci, B. Kachar, J. Gale, S. M. Van Netten, Mechano-electrical transduction: new insights into old ideas. *J Membr Biol* 209, 71-88 (2006).